Moist Physics Experiments in a Global Radiative-Convective Equilibrium Framework

A. R. Herrington and K. A. Reed

School of Marine and Atmospheric Sciences, Stony Brook University, NY

BACKGROUND

Variable and adaptive meshes represent a promising pathway towards improved regional climate projections in global models. However, global primitive equation models are notoriously non-convergent, resulting in diverging solutions across mesh transitions. It is generally thought that poorly formulated closure approximations are responsible for non-convergence in the models, however the specific mechanisms remain elusive. The idealized, non-rotating radiative-convective equilibrium (RCE) framework may be useful for isolating specific mechanisms leading to non-convergence in global atmospheric models (Reed et al 2015; Herrington and Reed 2016). Additionally, high horizontal resolution can be achieved through a reduction in planetary radius, which reduces computational costs at the expense of a reduced domain size (Reed and Medeiros 2016).

The RCE framework is applied to the joint DOE/ NCAR Community Atmosphere Model (CAM; Neale et al 2012) coupled to two different moist-physics packages: CAM version 5 physics (CAM5) and a developmental version of the anticipated CAM version 6 physics, containing the Cloud Layers Unified by Binormals closure (CLUBB; Golaz et al 2002). CLUBB serves as the PBL, shallow convection and cloud macrophysics scheme in our simulations, coupled with an updated version of CAM5 microphysics (Morrison and Gettleman 2015). All simulations were performed with the Spectral-Element dynamical core, which solves the adiabatic dynamics on a quasi-uniform cubed-sphere mesh (Figure 1).

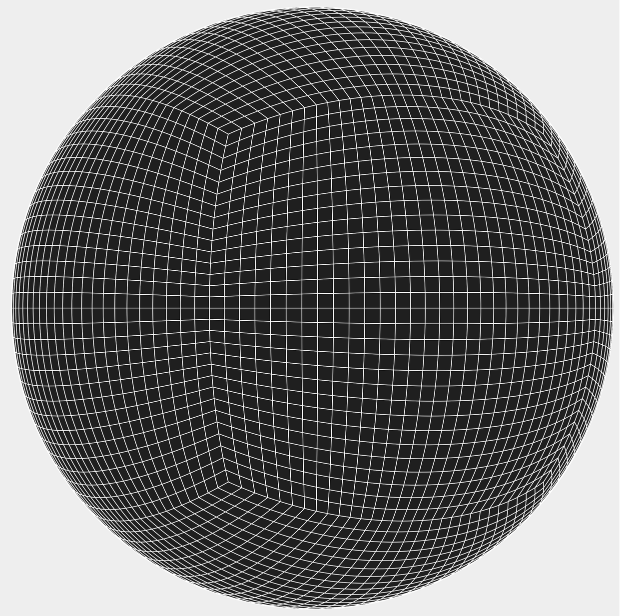

Figure 1. Cubed-sphere grid used in the study, Contains 30 elements along the edges of 6 square panels.

WHAT TO EXPECT

The RCE framework is non-rotating, and approximates the dynamical regime of the deep tropics. Let's take a look at the deep tropics in an aqua-planet run:

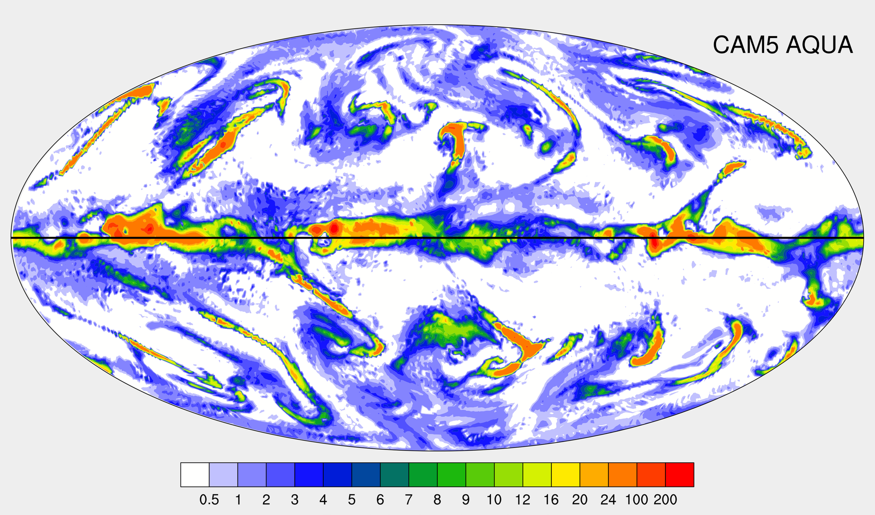

Figure 2. Snapshot of the total precipitation rate for an aqua-planet simulation at ~110 km using the CAM5 physics package.

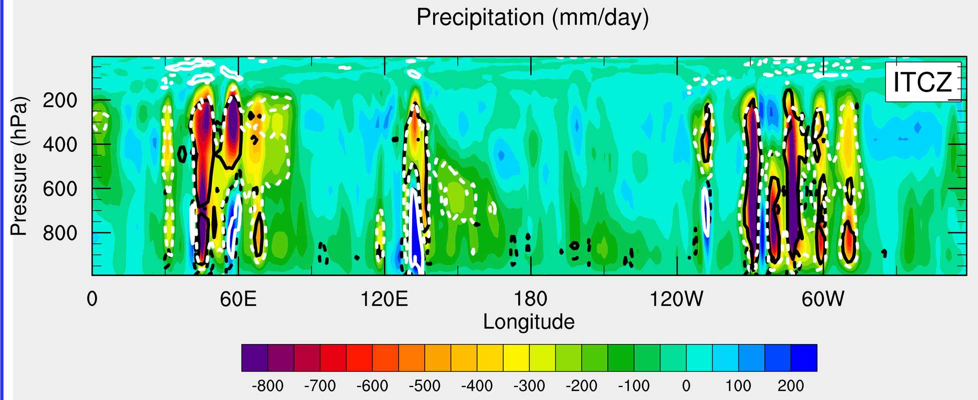

Figure 3. Longitude-height profiles of ω (colors) and temperature tendencies arising from the large-scale condensational scheme (black contours) and the dynamical core (white contours). Contour levels correspond to (-10, 10) K/d.

The diabatic forcing is the sum of temperature tendencies from the dynamical core and the physics package. We define a "resolved convective" forcing as the sum of large-scale condensational processes (black contours) and vertical advection of the background potential temperature field (white contours).

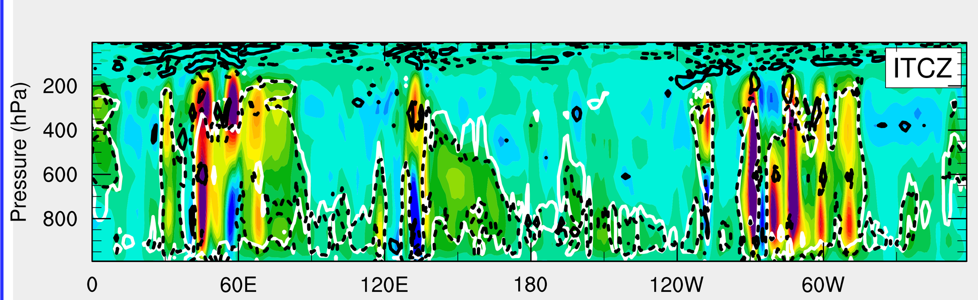

Figure X. Longitude-height profiles of ω (colors) and temperature tendencies from "resolved convection" (black contours) and parameterized convection (white contours). Contour levels are (-5, 5) K/d.

For strongly convecting systems, the "resolved" convective forcing (black contours) and parameterized convective forcing (white contours) occur together (Moncrieff and Klinker 1997).

GLOBAL DIAGNOSTICS

Table 1.

	CAM5 AQUA	CAM5	CAM5 small earth	CLUBB	CLUBB small earth	CAM5 no shallow	CLUBB delta
Internal + Potential Energy (x 10^7 J m^{-2})	256.05 (0.22)	265.76 (0.81)	269.14 (1.01)	262.57 (1.19)	266.38 (0.32)	265.01 (0.68)	263.4 (1.32)
Latent Energy (x 10^7 J m^{-2})	4.98 (0.04)	9.48 (0.6)	9.26 (0.84)	7.67 (0.74)	7.95 (0.73)	9.23 (0.48)	8.27 (0.85)
Kinetic Energy (x 10^5 J m^{-2})	25.95 (0.906)	1.874 (0.993)	0.434 (0.131)	0.415 (0.28)	0.534 (0.196)	0.915 (0.402)	0.568 (0.425)
$\lvert\omega(\omega < 0)\rvert$ (hPa d^{-1})	30.31 (49.31)	26.65 (49.45)	30.51 (101.98)	22.60 (42.56)	39.19 (152.48)	26.27 (43.65)	22.93 (37.62)
ZM Precipitation (mm d^{-1})	1.72 (0.081)	3.2 (0.51)	2.29 (0.58)	3.06 (0.53)	2.08 (0.64)	3.69 (0.63)	3.25 (0.61)
Total Precipitation (mm d^{-1})	3.16 (0.13)	3.89 (0.58)	4.6 (0.7)	3.28 (0.52)	4.26 (0.66)	3.79 (0.64)	3.44 (0.60)
Convective Ratio (ZM/Total)	0.54 (0.03)	0.82 (0.18)	0.5 (0.15)	0.93 (0.22)	0.49 (0.17)	0.97 (0.23)	0.95 (0.24)

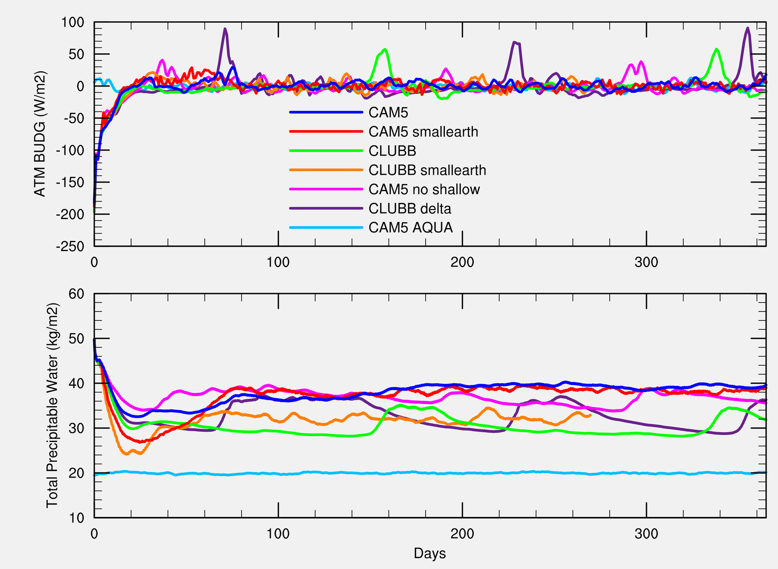

Figure 4. Globally averaged atmospheric energy budget (top) and latent energy (below) over time in the simulations.

In the RCE framework, the sea surface temperature is constant everywhere (302.15 K) and the solar angle is fixed with latitude (90˚). The boundary conditions provide tight constraints on the internal and potential energy (Table 1). CLUBB is generally drier than CAM5 (Table 1 and Figure 4), while other diagnostics show no clear distinction between the two physics packages. The simulations achieve RCE within two months (Figure 4). Periodic departures from RCE occur in the CLUBB simulations, reflecting occasional pulses of to a more aggregated, or CAM5-like state.

RCE SIMULATIONS (110 km)

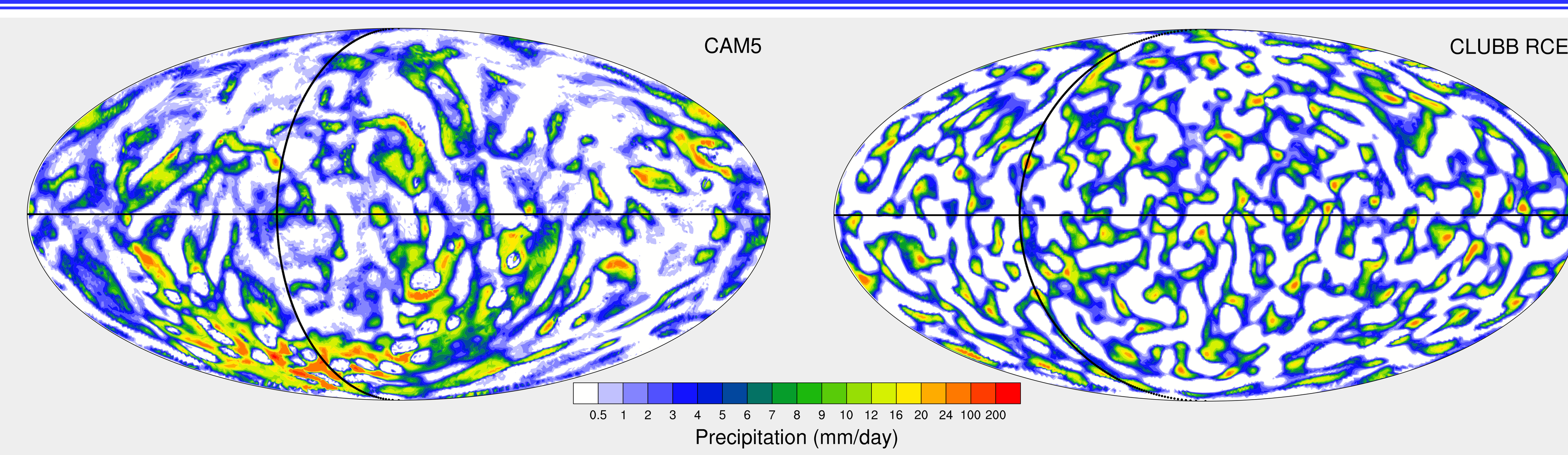

Figure 5. Snapshots of the total precipitation rate in the CAM5 and CLUBB RCE simulations.

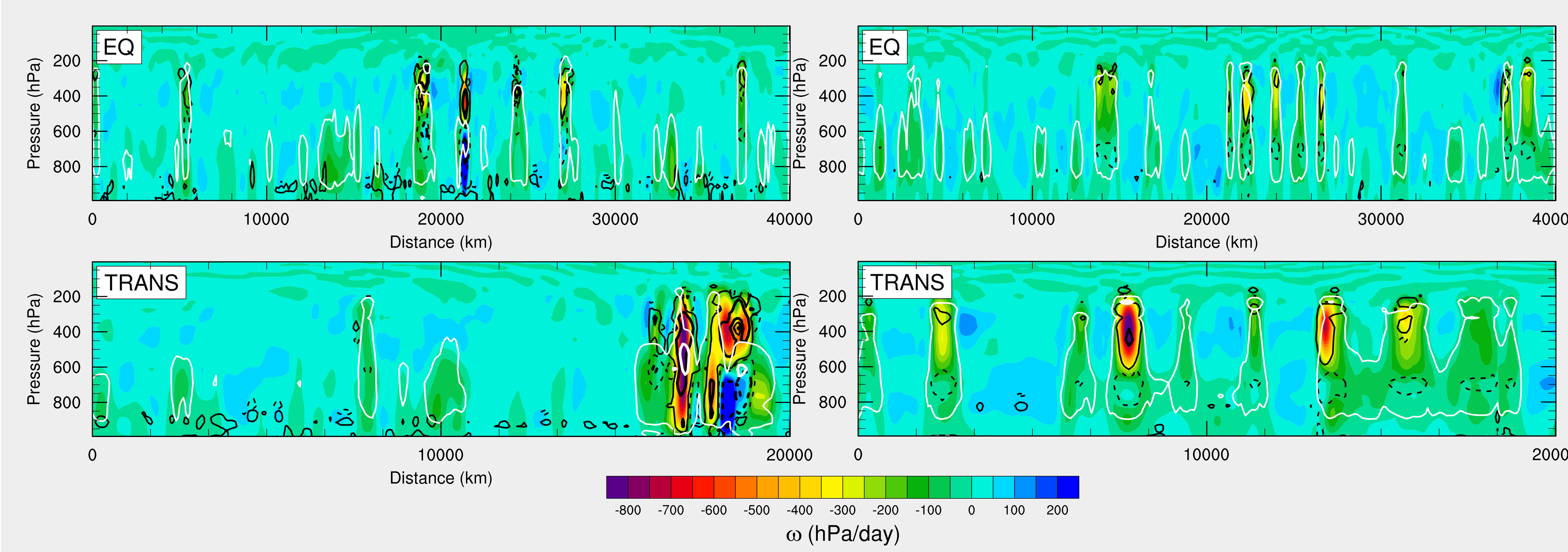

Figure 6. Pressure-distance plots (transects from Figure 5) of ω (color contours), with the parameterized deep convective forcing (white contours) and the forcing from the remaining parameterized moist processes (for the CLUBB simulations, this is equal to the sum of microphysics and CLUBB forcing). Contour levels correspond to (-20, -2, 2, 20) K/day, with negative values dashed.

REDUCED EARTH RCE SIMULATIONS (28 km)

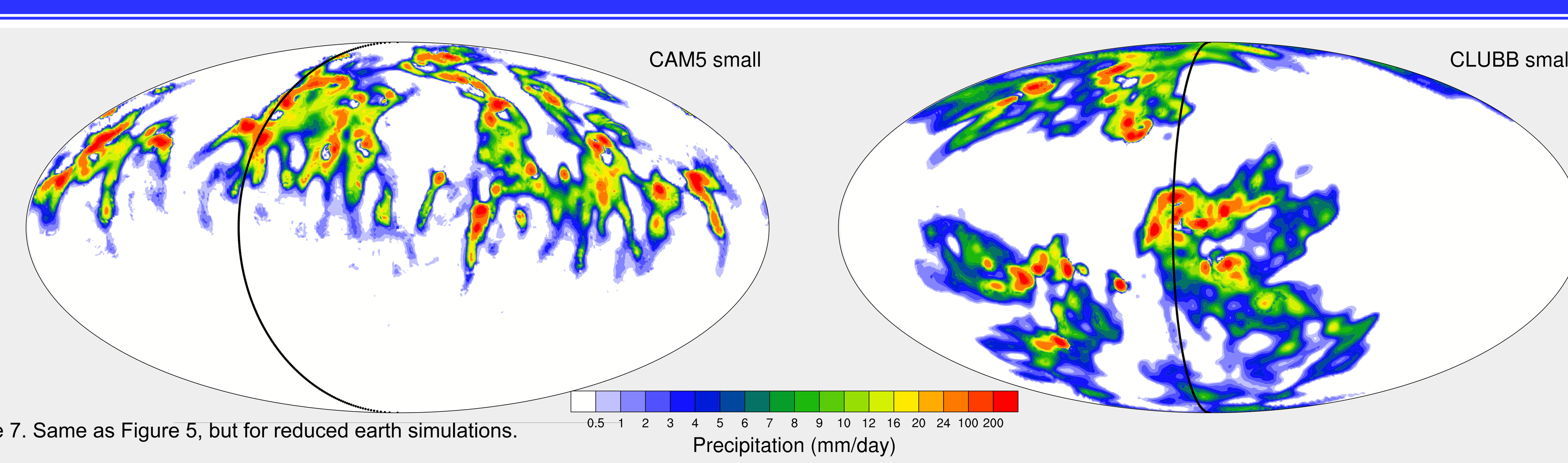

Figure 7. Same as Figure 5, but for reduced earth simulations.

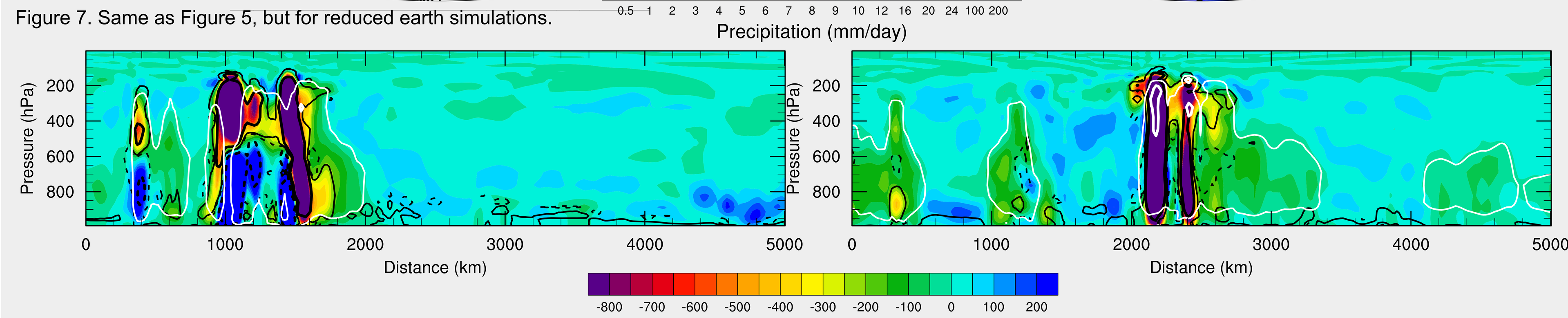

Figure 8. Same as Figure 6, but for reduced earth simulations.

CLUBB MACROPHYSICS

CLUBB's macrophysics solve for the grid scale condensation and cloud fraction using a spatially filtered density function for liquid water potential temperature that is approximated from the prognostic higher-order moments. Replacing the density function with a single dirac-delta function in the cloud fraction routine ("CLUBB delta") increases the occurrence of saturated air, with values intermediate to the CAM5 and CLUBB runs (Figure 9). The increased saturation state of air in CLUBB delta has little effect on the time mean global statistics, but there is a clear indication of an increase in variance (Table 1; Figure 4).

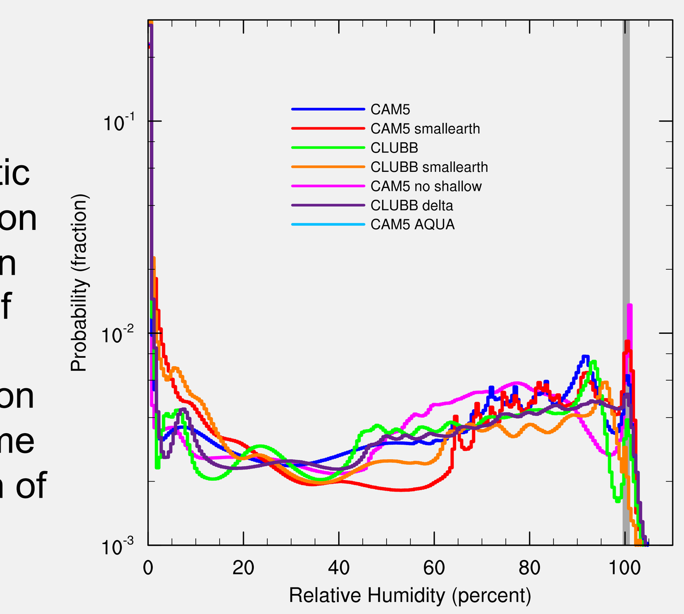

Figure 9. Probability density distributions of Relative Humidity. Data are from 180 days of 6-hour instantaneous output.

INTERPRETATION OF NON-CONVERGENCE

A reduction in planetary radius leads to a more aggregated state and stronger "resolved convection". While stronger "resolved convection" is likely related to the aggregated state, it is also predicted from a normal mode analysis of the Boussinesq equations (Weisman et al 1997). In the linear theory, a vertical velocity perturbation is unstable as the buoyancy frequency becomes negative. For the scales resolved in our simulations, k << m and the predicted unstable growth rate increases linearly with k.

The cross correlation coefficient, computed from instantaneous total physics tendencies and ω (Table 2), increases by 1.3X with the 4X reduction in planetary radius. The least-squares regression also predicts a ~1.3X increase in slope, indicating a higher sensitivity of ω per unit diabatic forcing with the reduced radius. Assuming the buoyancy frequency has some functional dependence on the diabatic forcing, the direction of the simulation statistics are consistent with linear theory. Non-linearity is also likely important, considering the large variations in horizontal resolution (and domain size) in our experiments.

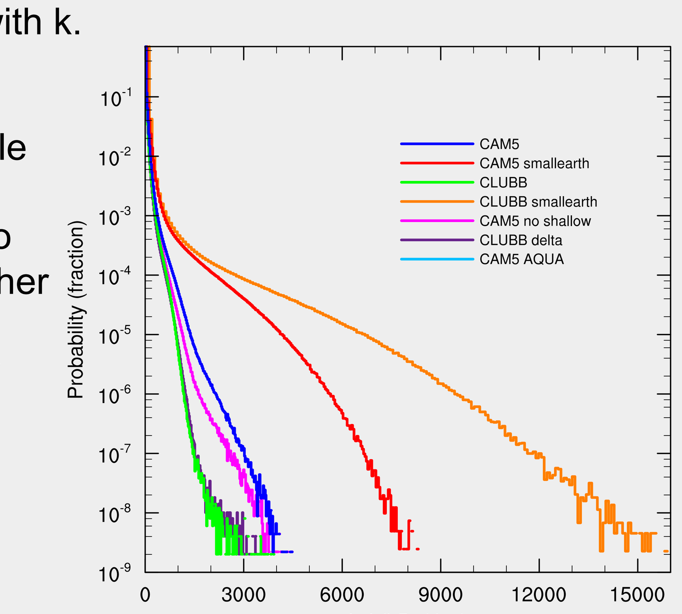

Figure 10. Probability density distributions of ω|(ω<0). Data are from 180 days of 6-hour instantaneous output.

	CAM5	CAM5 small earth	CLUBB	CLUBB small earth
Cross-correlation	-0.590	-0.842	-0.670	-0.935
Slope (hPa K^{-1})	-9.12	-14.34	-14.18	-19.70

Table 2. Regression statistics between ω and total physics tendency. Computed from instantaneous 6-hourly output over duration of respective simulations

Initially, we plan to investigate these issues in a dry framework and formulate a strategy for convergent solutions across mesh transitions. Next, we will perform climate simulations with Community Earth System Model using variable-resolution meshes, to investigate regional scale process and future climate impacts.

REFERENCES

Gettelman, A. and Coauthors (2015) "Advanced two-moment bulk microphysics for global models. Parth II: global model solutions and aerosol-cloud interactions." *Journal of Climate*, **28**, 1288-1307.

Golaz, J. C., Larson, V. E. and W. R Cotton (2002) "A PDF based model for boundary-layer clouds. Part I: Method and Model description." *Journal of the Atmospheric Sciences*, **59**, 3541-3551.

Herrington, A. R. and K. A. Reed (2016) "On the non-convergence of the Community Atmosphere Model with increasing resolution." *in revision*.

Neale, R. B. and Coauthors (2012) "Description of the NCAR Community Atmosphere Model (CAM 5.0)." NCAR Tech. Note NCAR/TN+486+STR, 268 pp.

Moncrieff, M. W. and E. Klinker (1997) "Organized convective systems in the tropical west Pacific as a process in general circulation models: A TOGA COARE case-study. *Q. J. R. Meteorol.* Soc., **123**, 805-827.

Reed, K. A. and B. Medeiros (2016) "A reduced complexity framework to bridge the gap between AGCMs and cloud-resolving models." *Geophysical Research Letters*, **42**, doi: 10.1002/2015GL066713.

Reed, K. A., B. Medeiros, J. T. Bacmeister and P. H. Lauritzen (2015) "Global radiative-convective equilibrium in the Community Atmosphere Model, version 5." *Journal of the Atmospheric Sciences*, **72**, 2183-2197.

Weisman, M. L. Skamarock, W. C. and J. B. Klemp (1997) "The resolution dependence of explicitly modeled convective systems." *Monthly Weather Review*, **125**, 527-548

Research supported through a NCAR small university allocation. CISL Project Number UNSB0009